

RESEARCH

Open Access



Non-targeted metabolomic profile of *Leuconostoc mesenteroides*-fermented milk reveals differentially expressed metabolites associated with electro-fermentation

Tristan Yusho Huang^{1*} and John Jackson Yang²

Abstract

Background *Leuconostoc mesenteroides* (*L. mesenteroides*) has known as an electrogenic probiotic bacterium. However, metabolites related to electro-fermentation in ferments of *L. mesenteroides* are not unveiled.

Result Electrogenic *L. mesenteroides* fermentatively metabolized bovine milk to dense ferments with homogeneous particle-size distribution. A non-targeted metabolomics approach was performed on non-fermented and *L. mesenteroides*-fermented milk. A total of 917 metabolites were identified and quantified by ultra-high performance liquid chromatography (UHPLC)-tandem mass spectrometry (MS-MS). Thirteen prokaryotic metabolic pathways associated with differentially expressed metabolites (DEMs) were revealed through Koto Encyclopedia of Genes and Genomes (KEGG) enrichment analysis. Anthranilic acid (AA) and 3-hydroxyanthranilic acid (3-HAA), potentially as electron donors, and quinolinic acid, an electron donor precursor, in the tryptophan kynurenine pathway were significantly increased in the fermented milk. Histidine, arginine, and riboflavin involved in bacterial survival or bioelectricity production were elevated after fermentation.

Conclusions Results indicate that electrogenic *L. mesenteroides* can mediate electro-fermentation to transform milk to a new nutritional source which is rich in electron donors reportedly acting as antioxidants.

Keywords Electrogenic, Kynurenine pathway, *Leuconostoc mesenteroides*, Milk ferments, Non-targeted metabolomic

Introduction

Leuconostoc mesenteroides (*L. mesenteroides*) is a Gram-positive and heterofermentative lactic acid probiotic bacterium which can mediate fermentation to produce several beneficial metabolites including short-chain fatty acids (SCFAs) [1]. It has been documented that butyric acid, one of SCFAs in glucose ferments of *L. mesenteroides*, efficiently elevated the level of insulin to ameliorate diabetes [2], and diminish high fat diet (HFD)-induced abdominal fat [3] via activation of free fatty acid receptor 2 (Ffar2) in mice. Notably, *L. mesenteroides* has been found as an electron-producing bacterium which

*Correspondence:

Tristan Yusho Huang
tristan.huang@midwestern.edu

¹Arizona College of Osteopathic Medicine, Midwestern University, Arizona 85308, USA

²Department of Medical Biochemistry, Universitas Kristen Indonesia, Jakarta 13630, Indonesia



© The Author(s) 2025. **Open Access** This article is licensed under a Creative Commons Attribution-NonCommercial-NoDerivatives 4.0 International License, which permits any non-commercial use, sharing, distribution and reproduction in any medium or format, as long as you give appropriate credit to the original author(s) and the source, provide a link to the Creative Commons licence, and indicate if you modified the licensed material. You do not have permission under this licence to share adapted material derived from this article or parts of it. The images or other third party material in this article are included in the article's Creative Commons licence, unless indicated otherwise in a credit line to the material. If material is not included in the article's Creative Commons licence and your intended use is not permitted by statutory regulation or exceeds the permitted use, you will need to obtain permission directly from the copyright holder. To view a copy of this licence, visit <http://creativecommons.org/licenses/by-nc-nd/4.0/>.

metabolizes glucose [1] or linoleic acid [3] to generate electrons through an intracellular cyclophilin A-dependent pathway. Electron produced by linoleic acid fermentation of *L. mesenteroides* remarkably suppressed the formation of HFD-induced 4-hydroxy-2-nonenal (4-HNE), an end product of lipid peroxidation and a biomarker of free radicals [3].

Electrogenic bacteria undergo a mechanism of extracellular electron transfer (EET) to transfer intracellular electron to its acceptor outside of the bacteria [4]. One of pathways of EET involves in activation of type II nicotinamide adenine nucleotide (NADH) dehydrogenase (NDH-2) to oxidize NADH generated by glycolysis or fermentation, and yield nicotinamide adenine dinucleotide (NAD⁺) as well as electron. Demethylmenaquinone-8 (DMK-8) on the membrane functions as an electron mediator to further transport electron to the extracellular space [5]. Electrogenic bacteria using EET have been identified in environment [6] and human gut [7] and skin [8]. In the human gut microbiome, it has been unveiled that bacterial EET well contributed to the potential balance of oxidation and reduction (redox) [9]. Inflammatory bowel diseases (IBD) induced excessive production of reactive oxygen species (ROS) in the intestine [10]. Likewise, antibiotic administration interrupted intestinal redox homeostasis [11]. Administration of electrogenic probiotic bacteria such as *Lactobacillus plantarum* (*L. plantarum*), *L. casei*, and/or *L. rhamnosus* [12] remarkably restored intestinal redox homeostasis by scavenging ROS [13] and simultaneously outcompeting with pathogens for electron acceptors [14]. These probiotic bacteria have been used to improve IBD [15] and help restore the gut microbiome after antibiotic disruption [16].

A fundamental intrinsic problem at conventional fermentation is associated with the need for balancing the net redox between substrates and fermentation products, resulting in a limited number of fermentation products being produced. One solution for this problem is electro-fermentation, a biotechnological process that uses electrodes to modify the cultural media by changing the redox balance in bacterial metabolism, resulting in the additional yields of fermentation products [17]. Electrogenic bacteria exerted EET to interact electrically with extracellular conductive substances [18]. When the continued generation of electrons by electrogenic bacteria occurs during fermentation, an adequate amount of electrons may overcome the redox constraint of fermentation, leading to production of sufficient bioelectricity and metabolites [19]. It has been illustrated that electrogenic *L. plantarum* can mediate EET to enhance fermentation metabolism through substrate-level phosphorylation and a decrease the extracellular pH [12]. ATP-binding cassette (ABC) transporters in bacteria are protein complexes which transfer specific molecules such as amino

acids across the cell membrane [20]. Certain types of ABC transporters accelerate the electron production in bacteria by facilitating the transport of amino acids such as histidine that is involved in EET [21], assisting the process of electron generation.

Bovine milk is a very ample source of amino acids including phenylalanine and tryptophan [22]. Previous studies using targeted metabolite analysis revealed thatelectrogenic *L. mesenteroides* metabolized phenylalanine to various neurotransmitters [23]. Tryptophan can be metabolized by bacteria through several pathways including serotonin, indole and kynurenine pathways [24]. Future foods are developing proteins that can be synthesized using gas, light or electrons [25]. Carbon dioxide (CO₂) fermentation is a method of eco-fermentation where bacteria convert CO₂ into value-added molecules [26, 27]. In this study, we aimed to determine which metabolic pathways were utilized by electrogenic bacteria to yield valuable metabolites. Electrogenic *L. mesenteroides* was used as a probiotic bacterium for fermentation of bovine milk. A non-targeted metabolite analysis using ultra-high performance liquid chromatography (UHPLC)-tandem mass spectrometry (MS-MS) was performed to quantify the metabolites in fermented milk.

Materials and methods

Bacterial growth

The curd during making cheese from products in the New England Cheesemaking Supply Company (Northampton, MA, USA) was spread on an agar (0.3%) plate containing tryptic soy broth (TSB) (Sigma, St. Louis, MO, USA) for 24 h. A bacterial colony was selected from the agar plate and cultured in TSB at 37 °C for 24 h. After centrifugation at 5,000 rpm for 10 min, bacterial pellets were resuspended in phosphate-buffered saline (PBS) for all experiments. The colony forming units (CFUs) of bacteria were calculated by conversion of optical density 600 nm (OD₆₀₀) to bacterial numbers.

Gram staining and catalase test

For Gram staining, pellets of bacteria (10⁷ CFU/mL) were resuspended by a Gram stain kit (Sigma) and spread evenly across the surface of a microscope slide. Catalase tests were conducted by placing 3% H₂O₂ (100 μL) onto bacteria (5 × 10⁶ CFU) on glass slides [28]. The bubbles leading from production of oxygen gas indicated a catalase positive result.

Phylogenetic analysis

Identification of bacteria were conducted by 16 S rRNA sequencing using the 16 S rRNA 27 F and 534R primers for polymerase chain reaction (PCR) [8]. The basic local alignment search tool (BLASTN, National Library

of Medicine 8600 Rockville Pike, Bethesda, MD, USA) was used to analyze the 16 S rRNA gene sequence of a selected colony. The gene sequences of 16 S rRNA from selected colony and other bacteria were uploaded onto ClustalW [29], an algorithm for multiple sequence alignment (MSA). A phylogenetic tree was created by Molecular Evolutionary Genetics Analysis (MEGA), a software that implemented many analytical methods and tools for phylogenetic analysis [30]. The bootstrap values were calculated from 1,000 replicate datasets to obtain the confidence level of each branch on a phylogenetic tree.

Fermentation

For milk fermentation, the identified *L. mesenteroides* bacteria (10^8 CFU/mL) were added into the whole bovine milk (Agropur, Appleton, WI, USA) at 37 °C for three days. The formation of dense solids during milk fermentation was recorded every 6 h. The freeze-dried powders were prepared by placing fermented milk in Eyela laboratory freeze-dryer (Eyela USA, NY, USA) under a vacuum pressure of 100 millitorrs for 12 h [23].

Bacterial electricity and physicochemical characteristics of milk ferments

Detection of bacterial electricity was based on a published method [31]. Briefly, *L. mesenteroides* (10^7 CFU) in 2 mL TSB with or without 2% glucose (Sigma) was placed onto a carbon felt (Fuel Cell Earth LLC, Woburn, MA, USA) as anode. A carbon cloth (Fuel Cell Earth LLC) wrapped with a proton exchange membrane (PEM) served as a cathode. Change in voltage (mV) was recorded for 60 min by a digital multimeter (Lutron, DM-9962SD, Sydney, Australia). The particle sizes analyzed by dynamic light scattering and zeta potentials evaluated by an electrophoretic mobility technique were performed by a Malvern Mastersizer 3000 and a Zetasizer Nano ZS, respectively (Malvern Panalytical Inc., Westborough, MA, USA) [32]. All analyses were run in triplicate at room temperature (20 ± 1 °C) after diluting (1:50) the freeze-dried powders with distilled water.

Non-targeted metabolite analysis

The freeze-dried powders (50 mg) were dissolved in 150 μ L of 50% methanol (containing 5 ppm 2-chlorophenyl-alanine). After centrifugation at 12,000 rpm, the supernatant was filtered through a 0.22 μ m filter membrane and mixed with quality control (QC) samples for evaluating instrument stability. For non-targeted UHPLC-MS-MS analysis [33], an Orbitrap Exploris 120 mass spectrometer (ThermoFisher Scientific, Greenville, NC, USA) was connected to a Vanquish UHPLC (ThermoFisher Scientific) to identify the metabolites in non-fermented and fermented milk. An ACQUITY UPLC HSS T3 column (Waters Corporation, Milford, MA, USA) in the UHPLC

system was used with a flow rate of 0.4 mL/min. Formic acid (0.1%) and acetonitrile (containing 0.1% formic acid) were selected for mobile phase A and B, respectively. The mass spectrometer with Xcalibur software (version: 4.7, Thermo) was used to obtain data-dependent acquisition (DDA) data. Heated electrospray ionization (HESI) source was operated to obtain a resolution of 60,000, via scan range 100–1000 mass-to-charge ratio (m/z), automatic gain control (AGC) Target Standard, and Max IT 100 ms. The top 4 ions were screened for secondary fragmentation to attain a resolution of 15,000 via higher energy collision dissociation (HCD) energy 30%, AGC Target Standard and Max IT Auto.

Metabolite library search and quantification

The new generation commercial software Compound Discoverer™ 3.3 (version 3.3.2.31, Thermo, Waltham, USA) combined with various types of MS-MS spectral libraries was used to perform qualitative and quantitative analysis of metabolites. The peaks in MS-MS spectra that were undetected in more than 50% of the QC samples were filtered, and the miss values of the undetected peaks were filled using the software Fill Gaps algorithm, and the Sum total peak area was then normalized. The mzCloud online library (<https://www.mzcloud.org/>), LIPID MAPS (<https://www.lipidmaps.org/>), human metabolome database (HMDB) (<https://hmdb.ca/>), MoNA (<https://mona.fiehnlab.ucdavis.edu/>) and NIST_2020_MSMS spectral library [34] served as sources for identification of metabolites. The mass tolerance of the first stage of mass spectrometry (MS1) was set to 15 ppm and the Match Factor Threshold of the second stage of mass spectrometry (MS2) was set to 50. Metabolites with p-value < 0.05 and various important in projection (VIP) > 1 were considered statistically significant (Table S1). The relative abundance of metabolites in non-fermented milk and fermented milk was shown in a Volcano plot. Metabolites with the magnitude of the fold change in binary logarithm [$\log_2(\text{FC})$] by combining the statistical t-test [$-\log_{10}(\text{p value})$] were displayed.

Pathway analysis

Functional examination of differential metabolites by clusterProfiler (version 4.6.0) mainly involved Koto Encyclopedia of Genes and Genomes (KEGG) enrichment analysis [35], which displayed significantly enriched metabolic pathways and measured overall differential abundance scores to reveal the average and overall trend changes of all differential metabolites within a specified pathway, assisting in the identification of metabolic pathways in bacteria. The differentially expressed metabolites (DEMs) were quantified and displayed in the specified pathways. The p-value ranged from 0 to 1 was shown in KEGG pathway enrichment. A lower p-values indicated

greater pathway enrichment. The rich factor was the ration of differentially expressed metabolite numbers annotated in the pathway to all metabolite numbers marked in the ways. The greater the rich factor was obtained, the greater the degree of pathway enrichment was considered (Table S2).

Statistical analysis

The unpaired t-test using GraphPad Prism® 8.0 software was performed for statistical analysis. Results were considered statistically significant when the *p*-values of <0.05 (*), <0.01 (**), and <0.001 (***). The mean ± standard deviation (SD) was calculated from data obtained from at least three independent experiments.

Results

Biochemical characteristics and phylogenetic analysis of 16 S rRNA gene sequence of selected *L. mesenteroides*

A bacterium colony isolated from cheese appeared purple-violet and formed spherical or cocci-shaped cells under a microscope after a procedure of Gram positive stains (Fig. 1A). In a catalase test, no oxygen gas was produced from H₂O₂ reaction, indicating that selected bacteria did not express catalase (Fig. 1B). The 16 S rRNA gene sequence of a selected colony shared 99.80% identity to 16 S ribosomal RNA gene, partial sequences for *L. mesenteroides* strain American Type Culture Collection (ATCC)8293T [accession identification (ID): KX886793], *L. mesenteroides* strain SJRP174 (accession ID: MH698390) isolated from whey, *L. mesenteroides* strain

TA (accession ID: KU361186) isolated from kimchi, and *L. mesenteroides* subsp. 213M0 dextranicum gene (accession ID: AB97900) isolated from Mongolian fermented mare milk. In addition, the 16 S rRNA gene sequence of a selected colony had 96.74% and 97.10% identity to *Leuconostoc lactis* (*L. lactis*) strain MBFCND-13 (accession ID: GU049408) and strain Korean Collection for Type Cultures (KCTC)3528 (accession ID: LC071838), respectively (www.arb-silva.de). A phylogenetic tree showed that four *L. mesenteroides* strains (ATCC8293T, SJRP174, TA and 213M0) located at different branches from two *L. lactis* strains (MBFCND-13 and KCTC3528). Furthermore, the identified *L. mesenteroides* had shorter branch distances to *L. mesenteroides* ATCC8293T, ATCC8293T, SJRP174, TA or 213M0 strains and longer branch distances to two *L. lactis* strains, demonstrating a close evolutionary relationship of identified *L. mesenteroides* with other *L. mesenteroides* strains (Fig. 1C).

Bacterial electrogenicity and physicochemical characteristics of milk ferments

To confirm the electrogenicity of a *L. mesenteroides* strain isolated from cheese, electron-induced voltage changes from bacteria in the presence or absence of glucose were measured in vitro using electrodes. As shown in Fig. 2A, *L. mesenteroides* in media with glucose triggered a higher voltage change compared to bacteria in media without glucose, supporting previous results that *L. mesenteroides* was an electrogenic bacterium which can metabolize glucose to yield electrons [1]. To investigate the probiotic

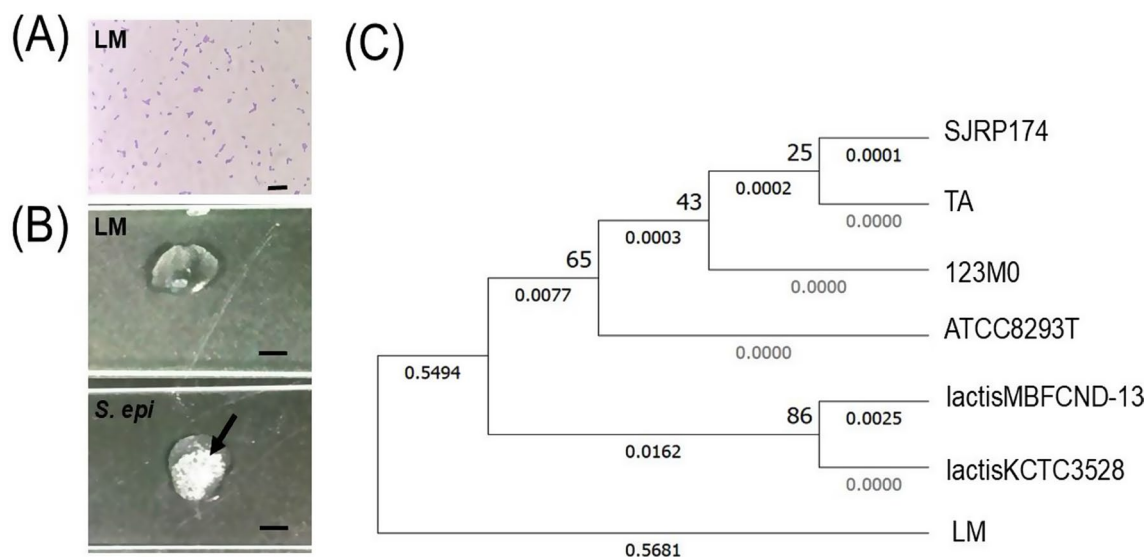


Fig. 1 Biochemical characteristics and phylogenetic analysis of selected *L. mesenteroides* bacteria. **(A)** Gram positive stains showed the bacteria had purple-violet appearance and formed spherical or cocci-shaped cells. Bar = 10 μ m. **(B)** Bubbles (arrow) leading from production of oxygen gas from *S. epidermidis* ATCC12228, a catalase positive bacterium, not but from identified *L. mesenteroides* (LM), a catalase negative bacterium. Bars = 0.5 cm. **(C)** A phylogenetic tree was constructed using the 16 S rRNA gene sequences from identified *L. mesenteroides* (LM), four *L. mesenteroides* strains (ATCC8293T, SJRP174, TA and 213M0) and two *L. lactis* strains (MBFCND-13 and KCTC3528). Bootstrap values based on 1,000 replications were indicated at branch nodes. The branch length, representing the amount of evolutionary change or genetic divergence, was shown

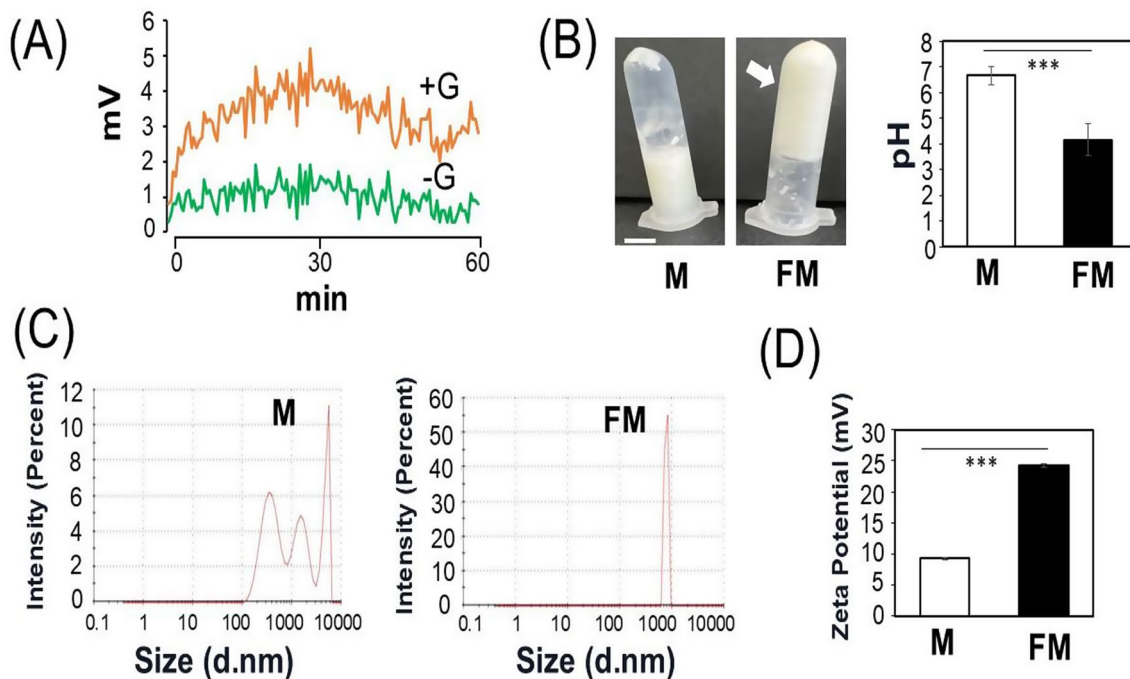


Fig. 2 Particle sizes and zeta potentials in *L. mesenteroides*-fermented bovine milk. **(A)** Bacterial electricity measured by voltage changes (mV) was recorded for 60 min in the presence (+G) or absence (-G) of glucose. **(B)** The formation of dense solid (arrow) and pH values were observed in fermented milk (FM), not non-fermented milk (M). Bar = 0.5 cm. **(C)** Particle sizes (d.nm; diameter in nanometers) and zeta potentials (mV) **(D)** of non-fermented milk (M) and fermented milk (FM) were compared. The p -values of < 0.001 (***) with mean \pm SD from experiments in triplicate were displayed

activity of *L. mesenteroides*, bacteria were incubated with bovine milk. The formation of dense solid in bovine milk and a reduction in pH values from 6.66 ± 0.35 to 4.50 ± 0.62 indicated the occurrence of fermentation after adding *L. mesenteroides* for 3 days (Fig. 2B). Different sizes of particles from 100 to 10,000 nm were detected in non-fermented milk. However, the particle sizes (approximately 1,000) in fermented milk became uniform after bacterial fermentation (Fig. 2C). Furthermore, the *L. mesenteroides* fermentation increased the absolute values of the negative zeta potentials of particles in milk from -9.24 ± 0.18 mV to -24.67 ± 0.25 mV (Fig. 2D).

Abundant metabolites in bovine milk and their changes after *L. mesenteroides* fermentation

The abundance of metabolites in milk was quantified based on their intensities of corresponding peaks on the MS-MS spectra. 917 metabolites were detectable through a non-targeted metabolite analysis using UHPLC-MS-MS (Table S1). Nine metabolites with intensities greater than 2×10^9 were detected in non-fermented milk (Fig. 3A). The content of linoleamide had no changes after fermentation. However, the content of leucyltryptophan, a dipeptide, in fermented milk had increased by 2.19-fold compared to non-fermented milk. The amounts of three amino acids or short peptides [phenylalanine-leucine (phe-leu), L-norleucine, and

H-proline-leucine-histidine-OH (H-pro-leu-his-OH)], three lipids (L-alpha-glycerol-phosphorylcholine, sphinganine, and choline) and palmitic acid reduced after fermentation. Results in Fig. 3A and Table S1 indicated that bovine milk contained various amino acids/short peptides, lipids and organic acids and their abundances can be changed by metabolism of *L. mesenteroides* during fermentation.

Metabolites with large magnitude changes and high statistical significance after milk fermentation

A volcano plot displays metabolites which have both statistically significant and large magnitude changes [36]. As shown in Fig. 3B, among 917 identified metabolites, 95 metabolites did not alter their abundances after fermentation. However, compared with metabolite abundance in non-fermented milk, 380 [$\log_2(\text{FC}) \geq 1$; $-\log_{10}(\text{p value}) \geq 1.3$] and 442 [$\log_2(\text{FC}) \leq -1$; $-\log_{10}(\text{p value}) \geq 1.3$] metabolites increased or decreased their contents, respectively, after fermentation. In fermented milk, the top 5 metabolites with a significant decrease were diethyl sulfate, perlargonidin, C20H34O4 {5-[4a,5-Bis(hydroxymethyl)-1,2-dimethyl-1,2,3,4,4a,7,8,8a-octahydro-1-naphthalenyl]-3-methylpentanoic acid}, daidzein, and genistein. The top 5 metabolites with a considerable increase were buprenorphine, LKK (H-lysine-leu-lysine-OH), L-isoleucyl-L-threonine, C40H61N7O8,

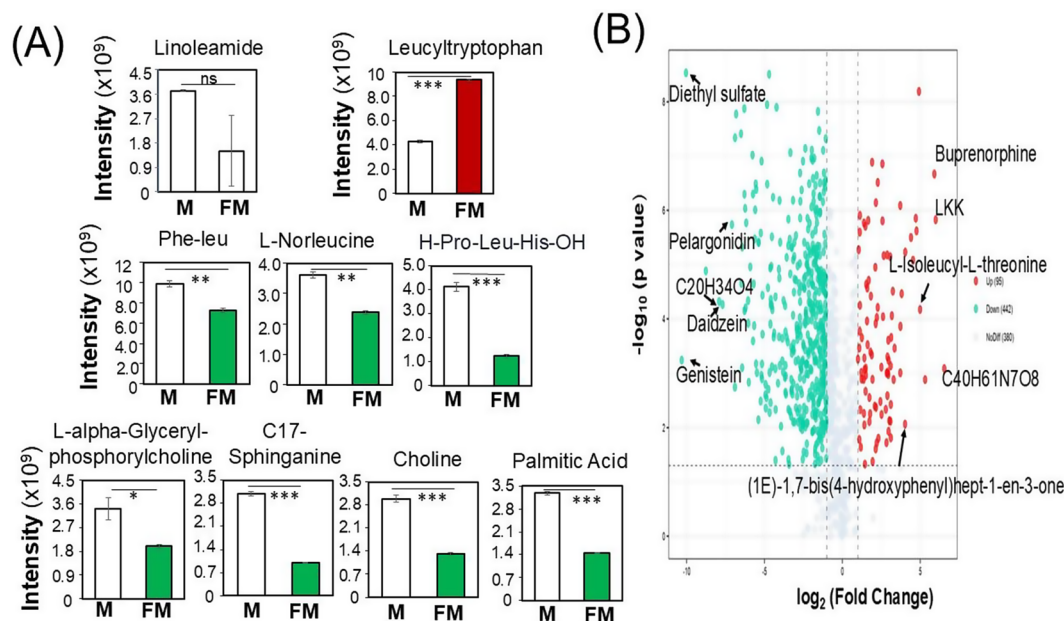


Fig. 3 Changes in the abundance of metabolites in *L. mesenteroides*-fermented bovine milk. **(A)** Changes of the nine most abundant metabolites with intensities $> 2 \times 10^9$ in mass spectra in non-fermented milk were quantified after *L. mesenteroides* fermentation. An increase (red), decrease (green) or no change (white) in abundance of metabolites after fermentation was displayed. A volcano plot **(B)** showed the relative changes of abundance of identified 917 metabolites. Red and green dots represented that the abundance of metabolites increased and decreased, respectively, in fermented milk. Grey dots indicated the rest of the metabolites with no significant changes that were detected in both non-fermented and fermented milk. The names of top 10 significantly changed metabolites (5 increased and 5 decreased metabolites) were shown. The *p*-values of < 0.05 (*), < 0.01 (**), and < 0.001 (***) from three separate experiments with mean \pm SD were shown. ns = non-significant

and (1E)-1,7-bis(4-hydroxyphenyl)hept-1-en-3-one. Pelargonidin, daidzein, and genistein are plant flavonoids which can be transferred to milk when they were added into the diet of lactating dairy ruminants [37, 38]. Although the volcano plot showed the top 10 significantly changed metabolites between non-fermented and fermented milk, the abundance of these metabolites in bovine milk was relatively low. In fact, several increased metabolites including trans-3-Indoleacrylic acid ($> 3.5 \times 10^8$ MS intensity; a 1.86-fold increase after fermentation) with high abundance and potential benefits for humans have been identified in fermented milk (Table S1). 122 of 380 increased metabolites with greater than a 1.5-fold increase after milk fermentation have been listed in Table S3.

Changed metabolites in metabolic pathways via KEGG enrichment analysis

The KEGG enrichment analysis showed that 200 changed metabolites, namely DEMs, between non-fermented and fermented milk were involved in 143 metabolic pathways. The top twenty pathways with the lowest *p*-values or the greatest pathway enrichment included seven eukaryotic and thirteen prokaryotic metabolic pathways. The thirteen prokaryotic metabolic pathways (Fig. 4, Table S2) in an order with *p*-values from low to high were ABC transporters (map02010), protein digestion and absorption

(map04974), biosynthesis of amino acids (map01230), aminoacyl-tRNA biosynthesis (map00970), mineral absorption (map04978), glycine, serine and threonine metabolism (map00260), cAMP signaling pathway (map04024), phenylalanine, tyrosine, and tryptophan biosynthesis metabolism (map00400), tryptophan metabolism (map00380), biosynthesis of cofactors (map01240), D-amino acid metabolism (map00470), beta-alanine metabolism (map00410) and citrate cycle (TCA cycle) (map00020). 16 DEMs were found in the pathway related to ABC transporters. The 6 (arginine, histidine, serine, adenosine, riboflavin and guanosine) out of 16 DEMs with increased abundance in the fermented milk. The rest of DEMs with decreased abundances were lysine, valine, maltose, uridine, isoleucine, 5-aminolevulinic acid, betaine, phthalic acid, xanthosine, and maltotriose (Table S2). The *p*-values, DEMs with increased/decreased abundance, and their associated KEGG WebLinks were shown in Table S2.

DEMs in the kynurenine pathway for tryptophan metabolism of *L. mesenteroides*

Results from the KEGG enrichment analysis (Fig. 4) have demonstrated that seven DEMs were associated with metabolism of tryptophan, which is particularly plentiful in milk. Tryptophan can be metabolized by probiotic bacteria through three major downstream pathways, the

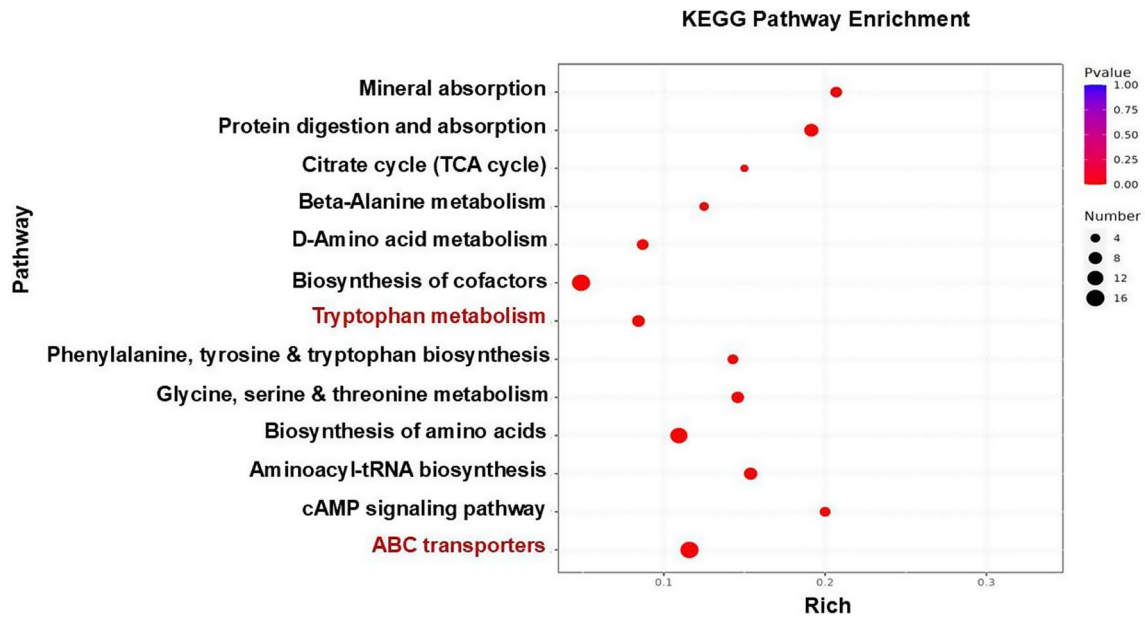


Fig. 4 The plot of KEGG enrichment pathway. After screening the DEMs in bovine milk after *L. mesenteroides* fermentation, thirteen prokaryotic metabolic pathways including tryptophan metabolism and ABC transporters) with lowest p-values (greatest pathway enrichment) were identified

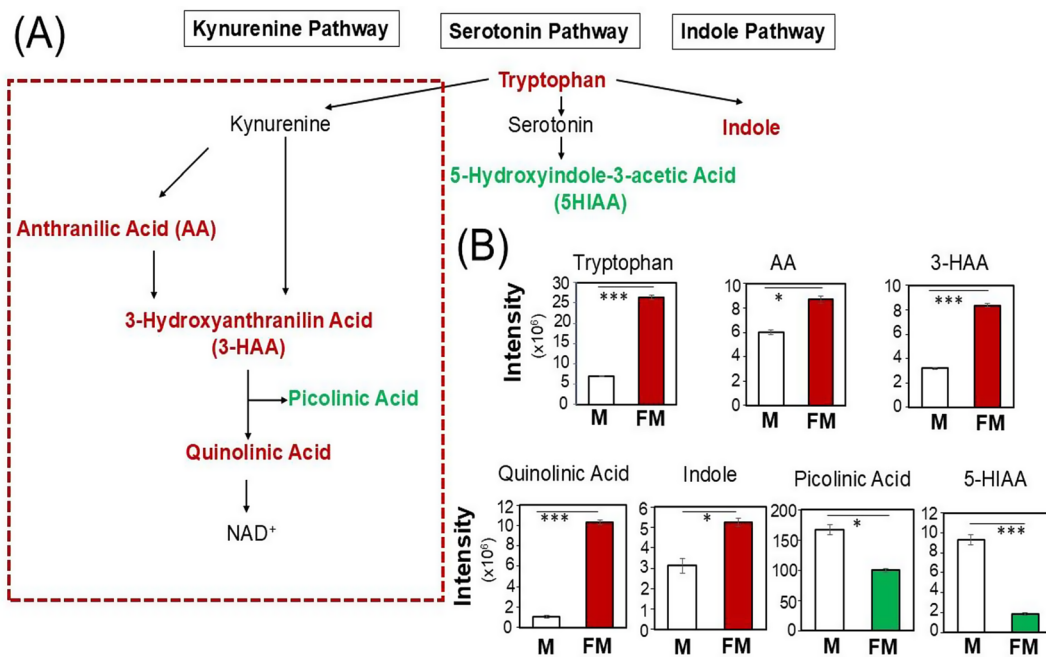


Fig. 5 Several metabolites involved in the kynurenine pathway augmented after *L. mesenteroides* fermentation. (A) Tryptophan in bovine milk was metabolized by *L. mesenteroides* to various metabolites via 3 different pathways (kynurenine, serotonin and indole pathways). (B) The abundance of five metabolites (tryptophan, AA, 3-AA, quinolinic acid, and indole) (red bars) significantly increased in fermented milk and the abundance of two metabolites (picolinic acid and 5-HIAA) (green bars) decreased in fermented milk (FM) compared to that in non-fermented milk (M) (open bars). The *p*-values of < 0.05 (*), and < 0.001 (***) from three different experiments with mean ± SD were shown

serotonin, indole, and kynurenine pathways (Fig. 5A). Five of seven DEMs including tryptophan, anthranilic acid (AA), 3-hydroxyanthranilin acid (3-HAA), quinolinic acid, and indole significantly increased their abundances in the *L. mesenteroides*-fermented milk (Fig. 5B).

Compared with non-fermented milk, the fermented milk contained lower amounts of 5-hydroxyindole-3-acetic acid (5-HIAA) and picolinic acid. A MS2 spectrum of quinolinic acid identified by UHPLC-MS-MS analysis was shown in Fig. 6. Remarkably, three DEMs (AA,

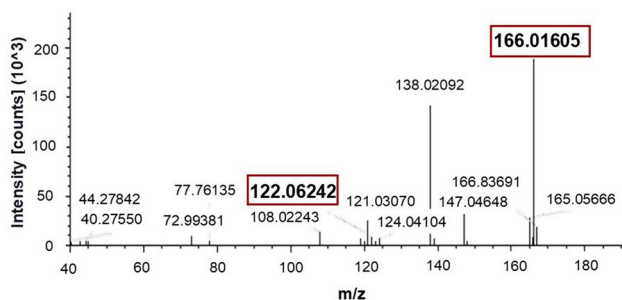


Fig. 6 The MS2 spectrum of quinolinic acid. UHPLC-MS-MS was performed to identify the quinolinic acid in *L. mesenteroides*-fermented milk. A peak at the retention time of 5.22 min in the UHPLC spectrum was subjected to MS-MS analysis. Two peaks (red squares) at MS2 spectrum with experimental m/z values at 122.0624 and 166.0160 well matched to theoretical m/z values at 122.0248 and 166.0146 of quinolinic acid, respectively

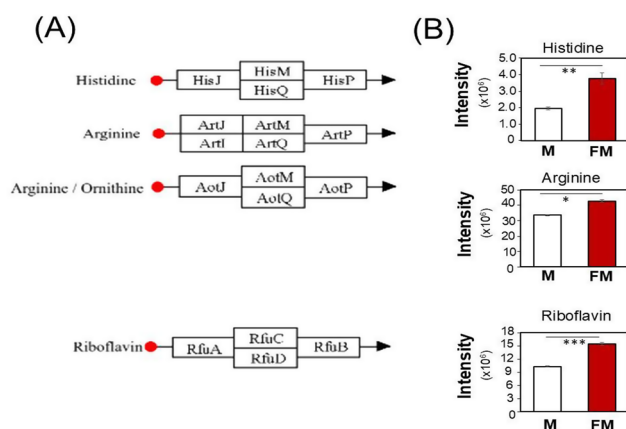


Fig. 7 The pathway of ABC transporters with the lowest p-values (greatest pathway enrichment) after screening DEMs. **(A)** The histidine transporter (HisPMQJ), arginine transporter (ArtJ-ArtPIQM), arginine/ornithine transporter (AotJ, Q, M and P), and riboflavin transporter (RfuABCD) were involved in translocation of histidine, arginine, arginine/ornithine, and riboflavin, respectively. **(B)** The levels of DEMs including histidine, arginine, and riboflavin in *L. mesenteroides*-fermented milk (FM) were significantly higher than those in non-fermented milk (M). The p-values of <0.05 (*), <0.01 (**), and <0.001 (***) and mean ± SD were obtained from experiments performed in triplicate

3-HAA, quinolinic acid) with elevated amounts in fermented milk indicated the activation of the kynurenine pathway in *L. mesenteroides* during fermentation. AA, 3-HAA and quinolinic acid have been known as an electron donor or precursor with properties of primary or secondary antioxidants [39, 40, 41] in the tryptophan kynurenine pathway, a route for cellular energy generation [42].

DEMs associated with prokaryotic-type ABC transporters

At least seven prokaryotic-type ABC transporters have been reported [43]. The KEGG enrichment analysis has linked sixteen DEMs to metabolic pathways of ABC transporters (Fig. 4 and Table S2). Phthalic acid and betaine were delivered across the bacterial membrane

through the mineral and organic ion transporters. Maltose, maltotriose and nucleosides (adenosine, guanosine, xanthosine, and uridine) which were mainly transported by basic membrane protein A (BmpA)-NupABC, were involved in the oligosaccharide, polyol, and lipid transporters. 5-aminolevulinic acid was transported by dipeptide-binding protein (Dpp)A which belonged to peptides and nickel transporters. Histidine, arginine, lysine, serine, valine and isoleucine mediated the phosphate and amino acid transporters across the bacterial membrane. Riboflavin can be delivered by riboflavin uptake (Rfu) ABC transporters which are the members of metallic cation, iron-siderophore and vitamin B12 transporters. As shown in Fig. 7, the amounts of histidine, arginine, and riboflavin were substantially increased after milk fermentation. *L. mesenteroides* is an electrogenic bacterium [1, 3]. The results have demonstrated that many metabolites with increased abundance after milk fermentation engaged in bacterial ABC transporters. The increased histidine, an electron donor [44], arginine, a pH regulator [45], and riboflavin, an electron amplifier [46, 47], may facilitate the survival or bioelectricity of *L. mesenteroides* during electro-fermentation.

Discussion

The non-fermented bovine milk contained heterogeneous sizes of particles (100 to 10,000 nm). After fermentation, particles in fermented milk became uniform in size at approximately 1,000 nm (Fig. 2C). Electrons generated by electrogenic *L. mesenteroides* may regulate the aggregation of casein micelles with negative surface charges in milk [48], resulting in homogeneous sizes of particles in fermented milk. A highly negative/positive zeta potential has been used to foresee the stability of particles [49]. High absolute values of zeta potentials indicated particle stabilities. As shown in Fig. 2D, the absolute value of zeta potentials of fermented milk was higher than that of non-fermented milk, suggesting that *L. mesenteroides* fermentation conferred good stability of milk ferments.

The relative abundance of metabolites in non-fermented milk or *L. mesenteroides*-fermented milk was determined by measuring the m/z of their ions in mass spectra (Fig. 3A). The abundance of metabolites was calculated based on their intensities of corresponding peaks on the mass spectra. Metabolites first were ionized by bombarding them with a high-energy electron beam to obtain their m/z values. However, not all metabolites, such as neutral metabolites, can be ionized readily, leading to signal loss. Several solutions including chemical derivatization [50] and ion suppression using ion-pairing agents [51, 52] have been proposed to quantify the poorly ionized metabolites in mass spectrometry. *L. mesenteroides* is a lactic acid bacterium with capability of converting lactose in milk to lactic acid. However, in

this study, lactic acid was not detected by non-targeted metabolite analysis. One of possible reasons may be due to the suppressive effects from other acids produced in fermented milk. Protons (H^+) derived from other acids may suppress the anion of lactic acid [53]. Furthermore, lactic acid is a relatively small and polar molecule which made identification difficult in ionization-required mass spectrometry. To accurately detect lactic acid in a complex fermentation mixture, specific sample preparation including derivatization [54] may be necessary to increase the efficiency of ionization. *L. mesenteroides* is a hetero-fermentative bacterium which can decompose the carbohydrates into multiple end products. Besides the metabolites with greater than 1.5-fold increased abundance (Table S3), many bioactive metabolites such as amino acids [glutamic acid (a 0.51-fold increase), phenylalanine (a 0.60-fold increase), and proline (a 0.57-fold increase)] and organic acids [citric acid (a 1.13-fold increase), malic acid (a 0.70-fold increase), and threonic acid (a 1.20-fold increase)] were detectable in milk fermentations of *L. mesenteroides*.

Cell-envelope proteinase (CEP) of lactic acid bacteria presents the activity in hydrolysis of milk proteins such as β -casein [55]. Milk fermentation by these bacteria has been known for generation of bioactive peptides (2–20 amino acid residues) with antioxidant properties [56]. Many short peptides among 917 metabolites (Table S1) have been identified in fermented milk although biological functions of these peptides are unknown. The amounts of phe-leu and H-pro-leu-his-OH peptides reduced after milk fermentation (Fig. 3A). Contrastingly, the levels of L-isoleucyl-L-threonine and LKK (H-lysine-leu-lysine-OH) increased after milk fermentation (Fig. 3B). Besides short peptides, organic acids were found abundantly in bovine milk. The content of trans-vaccenic acid, a fatty acid secreted in breast milk [57], was decreased after milk fermentation of *L. mesenteroides*. Compared to that in non-fermented milk, the abundance of trans-3-Indoleacrylic acid significantly increased in fermented milk. It has been reported that indoleacrylic acid eased type 2 diabetes via activation of the aryl hydrocarbon receptor (AhR) signaling pathway in rats [58]. However, the levels of 6-hydroxycaproic acid, hippuric acid, and phenyllactic acid (PLA), which affect the milk preservation [59, 60], were considerably reduced in fermented milk.

The kynurenine pathway is a metabolic route for breaking down tryptophan in both prokaryotes and eukaryotes, and it plays a critical role in generating cellular energy [42]. Although tryptophan catabolism through the kynurenine pathway in *L. mesenteroides* is not well characterized yet, three metabolites (AA, 3-HAA and quinolinic acid) in the kynurenine pathway were elevated by milk fermentation of *L. mesenteroides* (Fig. 5).

AA chemically is ortho aminobenzoate with electron-donating groups [61]. AA was viewed as a secondary antioxidant with application for inhibition of oxidative stress [62]. 3-HAA is an excellent electron donor in electrochemical experiments [63]. It can vastly reduce free radicals such as hydroxyl radical and peroxytrite [64] by hydrogen atom donation [65]. Quinolinic acid is a precursor of NAD^+ , an electron donor, and plays a critical role in oxidative phosphorylation and glycolysis [66]. Several Gram-positive bacteria express flavin synthesis genes and operate the flavin-based EET for electron transferring [47]. Riboflavin (vitamin B2), a precursor to the coenzymes flavin mononucleotide (FMN) and flavin adenine dinucleotide (FAD), secreted from bacteria can shuttle electrons to acceptors and amplify the electron signals [67]. Administration of FMN into an electrogenic bacterial culture led to a substantial increase in electric current [47]. As shown in Fig. 7A and Table S1, the amount of riboflavin in fermented milk was significantly higher than that in non-fermented milk. During electrofermentation, *L. mesenteroides* may mediate the catabolism of tryptophan in milk and/or flavin synthesis to enrich the amounts of AA, 3-HAA, quinolinic acid and riboflavin with the purpose of obtaining sufficient electron donors or mediators for sustaining its electrogenicity. Supplements of fermented milk with high amounts of electron donors or mediators may enhance energy production of human cells [68].

Through the KEGG pathway enrichment analysis, the increased and decreased metabolites in milk after fermentation were strongly related to ABC transporter pathway with the lowest p-value compared to that for other metabolic pathways (Table S2). The levels of histidine and arginine associated with histidine, arginine, arginine/ornithine transporters, respectively, were noticeably higher in fermented milk (Fig. 7). Histidine is an “electrogenic” amino acid with an imidazole ring structure, acting as an electron donor or acceptor. When interacting with metal ions like zinc or copper in active sites of enzymes, histidine can participate in electron transfer to influence the catalytic activities of enzymes [69]. Several histidine-rich motifs in DNA transcription factors, which take part in making the connection of proteins to nucleic acids by zinc-fingers [70]. It has been reported that histidine transporter is indispensable for bacterial growth under acid stress [71]. Furthermore, histidine electroactive bacteria have been identified [72]. These bacteria possess surface proteins containing histidine residues, functioning as a redox center, which can accept or donate electrons to participate in electrochemical reactions with their environment. It has been reported that bacteria can be genetically modified with histidine-tagged protein fibers to enhance their electroactivities [73]. Arginine or arginine/ornithine transporters facilitate the uptake

or exchange of arginine and ornithine across the bacterial membrane. *L. mesenteroides* expresses the arginine deiminase, which can convert arginine into ornithine and ammonia to protect bacteria from acidic environment [74]. Thus, the elevated histidine and arginine in fermented milk (Fig. 7) may increase the survival or electrogenic of *L. mesenteroides* during electro-fermentation.

Conclusions

The non-targeted metabolomics approach comprehensively profiled 917 metabolites in non-fermented and *L. mesenteroides*-fermented milk. The top 13 prokaryotic metabolic pathways included pathways related to ABC transporters and tryptophan metabolism, and ones with the lowest p-values were selected via KEGG enrichment analysis. The abundance of 3 DEMs (AA, 3-HAA and quinolinic acid) in the tryptophan kynurenine pathway and 3 DEMs (histidine, arginine, and riboflavin) associated with bacterial survival and EET substantially increased in *L. mesenteroides*-fermented milk. These DEMs may facilitate the electro-fermentation of *L. mesenteroides*. In addition, *L. mesenteroides*-fermented milk with these DEMs which acted as an electron donor or precursor may become new antioxidant nutrients for humans.

Abbreviations

| | |
|-------------------------|----------------------------------------|
| AA | Anthrannilic acid |
| ABC | ATP-binding cassette |
| AGC | Automatic gain control |
| AhR | Aryl hydrocarbon receptor |
| ATCC | American Type Culture Collection |
| BmpA | Basic membrane protein A |
| CEP | Cell-envelope proteinase |
| CFUs | Colony forming units |
| CO ₂ | Carbon dioxide |
| DDA | Data-dependent acquisition |
| DEMs | Differentially expressed metabolites |
| DMK-8 | Demethylmenaquinone-8 |
| DppA | Dipeptide-binding protein A |
| EET | Extracellular electron transfer |
| FAD | Flavin adenine dinucleotide |
| FC | Fold change |
| FDR | False discover rate |
| Ffar2 | Free fatty acid receptor 2 |
| FM | Fermented milk |
| FMN | Flavin mononucleotide |
| 3-HAA | 3-hydroxyanthranilic acid |
| HCD | Higher energy collision dissociation |
| HESI | Heated electrospray ionization |
| HFD | High fat diet |
| 5-HIAA | 5-hydroxyindole-3-acetic acid |
| his | histidine |
| HMDB | Human metabolome database |
| 4-HNE | 4-hydroxy-2-nonenal |
| IBD | Inflammatory bowel diseases |
| ID | Identification |
| KCTC | Korean Collection for Type Cultures |
| KEGG | Koto Encyclopedia of Genes and Genomes |
| leu | Leucine |
| <i>L. lactis</i> | <i>Leuconostoc lactis</i> |
| <i>L. plantarum</i> | <i>Lactobacillus plantarum</i> |
| <i>L. mesenteroides</i> | <i>Leuconostoc mesenteroides</i> |

| | |
|------------------|----------------------------------------------|
| MS-MS | Tandem mass spectrometry |
| MSA | Multiple sequence alignment |
| m/z | Mass-to-charge ratio |
| NADH | Nicotinamide adenine nucleotide |
| NDH-2 | NADH dehydrogenase 2 |
| NAD ⁺ | Nicotinamide adenine dinucleotide |
| OD | Optical density |
| PBS | Phosphate-buffered saline |
| PCR | Polymerase chain reaction |
| PEM | Proton exchange membrane |
| phe | Phenylalanine |
| PLA | Phenylactic acid |
| pro | Proline |
| QC | Quality control |
| Redox | Oxidation and reduction |
| ROS | Reactive oxygen species |
| Rfu | Riboflavin uptake |
| SCFAs | Short-chain fatty acids |
| SD | Standard deviation |
| TSB | Tryptic soy broth |
| UHPLC | Ultra-high performance liquid chromatography |
| VIP | Various important in projection |

Supplementary Information

The online version contains supplementary material available at <https://doi.org/10.1186/s12934-025-02673-5>.

Supplementary Material 1

Author contributions

T.Y.H. conducted experiment and wrote the main manuscript text and J.J.Y. provided bacterial strains and assisted non-targeted metabolomic analysis and revised manuscript. All authors reviewed the manuscript.

Funding

This work was supported by the research stipends of medical students obtained from Arizona College of Osteopathic Medicine, Midwestern University, USA.

Data availability

No datasets were generated or analysed during the current study.

Declarations

Ethics approval and consent to participate

Not applicable.

Consent for publication

Not applicable.

Competing interests

The authors declare no competing interests.

Received: 12 November 2024 / Accepted: 7 February 2025

Published online: 22 February 2025

References

- Yang JJ, et al. Production of electricity and reduction of high-fat diet-induced IL-6 by glucose fermentation of *Leuconostoc mesenteroides*. *Biochem Biophys Res Commun*. 2020;533(4):651–6.
- Traisang S, et al. *Leuconostoc mesenteroides* fermentation produces butyric acid and mediates Ffar2 to regulate blood glucose and insulin in type 1 diabetic mice. *Sci Rep*. 2020;10(1):7928.
- Pham MT, et al. *Leuconostoc mesenteroides* mediates an electrogenic pathway to attenuate the accumulation of abdominal fat mass induced by high fat diet. *Sci Rep*. 2020;10(1):21916.

4. Verma M, Singh V, Mishra V. Moving towards the enhancement of extracellular electron transfer in electrogens. *World J Microbiol Biotechnol.* 2023;39(5):130.
5. Pankratova G, et al. Extracellular Electron transfer by the Gram-positive bacterium *Enterococcus faecalis*. *Biochemistry.* 2018;57(30):4597–603.
6. Xiong X, Li Y, Zhang C. Cable bacteria: living electrical conduits for biogeochemical cycling and water environment restoration. *Water Res.* 2024;253:121345.
7. Tahernia M, et al. Characterization of Electrogenic Gut Bacteria. *ACS Omega.* 2020;5(45):29439–46.
8. Balasubramaniam A, et al. Skin Bacteria mediate glycerol fermentation to produce electricity and resist UV-B. *Microorganisms.* 2020;8(7):1092.
9. Zeng Z, et al. Bacterial microcompartments coupled with extracellular Electron transfer drive the anaerobic utilization of Ethanolamine in *Listeria monocytogenes*. *mSystems.* 2021;6(2):e01349–20.
10. Muro P, et al. The emerging role of oxidative stress in inflammatory bowel disease. *Front Endocrinol (Lausanne).* 2024;15:1390351.
11. Mu C, Zhu W. Antibiotic effects on gut microbiota, metabolism, and beyond. *Appl Microbiol Biotechnol.* 2019;103(23–24):9277–85.
12. Tejedor-Sanz S, et al. Extracellular electron transfer increases fermentation in lactic acid bacteria via a hybrid metabolism. *Elife.* 2022;11:e70684.
13. Feng T, Wang J. Oxidative stress tolerance and antioxidant capacity of lactic acid bacteria as probiotic: a systematic review. *Gut Microbes.* 2020;12(1):1801944.
10. Stevens E, Marco ML. Bacterial extracellular electron transfer in plant and animal ecosystems. *FEMS Microbiol Rev.* 2023;47(3):fud019.
15. Li C, et al. The role of *Lactobacillus* in inflammatory bowel disease: from actualities to prospects. *Cell Death Discov.* 2023;9(1):361.
16. Gao F, Fang Z, Lu W. Regulation divergences of *Lactobacillus fermentum* PCC and *Lactobacillus paracasei* 431 on penicillin-induced upper respiratory tract microbial dysbiosis in BALB/c mice. *Food Funct.* 2021;12(23):11913–25.
17. Kracke F, et al. Balancing cellular redox metabolism in microbial electrosynthesis and electro-fermentation - A chance for metabolic engineering. *Metab Eng.* 2018;45:109–20.
18. Logan BE, et al. Electroactive microorganisms in bioelectrochemical systems. *Nat Rev Microbiol.* 2019;17(5):307–19.
19. Sriram S, Wong JWC, Pradhan N. Recent advances in electro-fermentation technology: a novel approach towards balanced fermentation. *Bioresour Technol.* 2022;360:127637.
20. Akhtar AA, Turner DP. The role of bacterial ATP-binding cassette (ABC) transporters in pathogenesis and virulence: therapeutic and vaccine potential. *Microb Pathog.* 2022;171:105734.
21. Davidson AL, et al. Structure, function, and evolution of bacterial ATP-binding cassette systems. *Microbiol Mol Biol Rev.* 2008;72(2):317–64.
22. López-Diez L, et al. Amino acid metabolomic profiles in bovine mammary epithelial cells under essential amino acid restriction. *Anim (Basel).* 2021;11(5):1334.
23. Zhang M, et al. Neurotransmitter metabolites in milk ferments of *Leuconostoc mesenteroides* regulate temperature-sensitive heartbeats in an ex ovo model. *Heliyon.* 2024;10(16):e36129.
24. Miyamoto K, Sujino T, Kanai T. The tryptophan metabolic pathway of the microbiome and host cells in health and disease. *Int Immunol.* 2024;36(12):601–616.
25. Ciani M, et al. Microbes: food for the future. *Foods.* 2021;10(5):971.
26. Mishra S et al. Application of novel thermos-tolerant haloalkalophilic bacterium *Halomonas stevensii* for Bio mitigation of gaseous phase CO₂: Energy assessment and product evaluation studies. *Process Biochem.* 2017;55:133–45.
27. Ho SH, Chen WM, Chang JS. *Scenedesmus obliquus* CNW-N as a potential candidate for CO(2) mitigation and biodiesel production. *Bioresour Technol.* 2010;101(22):8725–30.
28. Taylor WI, Achanzar D. Catalase test as an aid to the identification of Enterbacteriaceae. *Appl Microbiol.* 1972;24(1):58–61.
29. Maulana H, et al. Bioinformatics study of phytase from *Aspergillus Niger* for use as feed additive in livestock feed. *J Genet Eng Biotechnol.* 2023;21:142.
30. Chen YS, et al. *Leuconostoc litchii* sp. nov., a novel lactic acid bacterium isolated from lychee. *Int J Syst Evol Microbiol.* 2020;70(3):1585–90.
31. Huang TY, Lim HL. Electrogenic *Staphylococcus warneri* in lactate-rich skin. *Biochem Biophys Res Commun.* 2022;618:67–72.
32. Alves E, et al. Characterization of Kefir Produced in Household conditions: Physicochemical and Nutritional Profile, and Storage Stability. *Foods.* 2021;10(5):1057.
33. Wang Z, et al. Non-targeted metabolomics of serum reveals biomarkers Associated with Body Weight in Wumeng Black-Bone Chickens. *Anim (Basel).* 2024;14(18):2743.
34. van der Laan T, et al. Data-Independent Acquisition for the quantification and identification of metabolites in plasma. *Metabolites.* 2020;10(12):514.
35. Yang T, et al. Untargeted metabolomics analysis of esophageal squamous cell cancer progression. *J Transl Med.* 2022;20(1):127.
36. Carlson AK, et al. Global metabolomic profiling of human synovial fluid for rheumatoid arthritis biomarkers. *Clin Exp Rheumatol.* 2019;37(3):393–9.
37. King RA, Bursill DB. Plasma and urinary kinetics of the isoflavones daidzein and genistein after a single soy meal in humans. *Am J Clin Nutr.* 1998;67(5):867–72.
38. Tian XZ, et al. Short communication: purple corn (*Zea mays* L.) stover silage with abundant anthocyanins transferring anthocyanin composition to the milk and increasing antioxidant status of lactating dairy goats. *J Dairy Sci.* 2019;102(1):413–8.
39. Halova-Lajoie B, et al. Copper (II) interactions with non-steroidal anti-inflammatory agents. III–3-Methoxyanthranilic acid as a potential *OH-inactivating ligand: a quantitative investigation of its copper handling role in vivo. *J Inorg Biochem.* 2006;100(3):362–73.
40. Thomas SR, Witting PK, Stocker R. 3-Hydroxyanthranilic acid is an efficient, cell-derived co-antioxidant for alpha-tocopherol, inhibiting human low density lipoprotein and plasma lipid peroxidation. *J Biol Chem.* 1996;271(51):32714–21.
41. Basbous H, et al. Transient formation of a second active site cavity during quinolinic acid synthesis by NadA. *ACS Chem Biol.* 2021;16(11):2423–33.
42. Dehghani M, et al. Microorganisms, Tryptophan Metabolism, and Kynurenine Pathway: a Complex interconnected Loop Influencing Human Health Status. *Int J Tryptophan Res.* 2019;12:1178646919852996.
43. Rice AJ, Park A, Pinkett HW. Diversity in ABC transporters: type I, II and III importers. *Crit Rev Biochem Mol Biol.* 2014;49(5):426–37.
44. Calinsky R, Levy Y. Histidine in proteins: pH-Dependent interplay between pi-pi, Cation-pi, and CH-pi interactions. *J Chem Theory Comput.* 2024;20(15):6930–45.
45. Agnello M, et al. Arginine improves pH Homeostasis via Metabolism and Microbiome Modulation. *J Dent Res.* 2017;96(8):924–30.
46. Lu M, et al. Effect of oxygen on the per-cell extracellular electron transfer rate of *Shewanella oneidensis* MR-1 explored in bioelectrochemical systems. *Biotechnol Bioeng.* 2017;114(1):96–105.
47. Light SH, et al. A flavin-based extracellular electron transfer mechanism in diverse Gram-positive bacteria. *Nature.* 2018;562(7725):140–4.
48. Liu Y, Guo R. Interaction between casein and the oppositely charged surfactant. *Biomacromolecules.* 2007;8(9):2902–8.
49. Bhattacharjee S. DLS and Zeta potential - what they are and what they are not? *J Control Release.* 2016;235:337–51.
50. Mantzourani C, Kokotou MG. Liquid Chromatography-Mass Spectrometry (LC-MS) derivatization-based methods for the determination of fatty acids in Biological samples. *Molecules.* 2022;27(17):5717.
51. Nshanian M, et al. Enhancing sensitivity of Liquid Chromatography-Mass spectrometry of peptides and proteins using Supercharging agents. *Int J Mass Spectrom.* 2018;427:157–64.
52. Mallet CR, Lu Z, Mazzeo JR. A study of ion suppression effects in electrospray ionization from mobile phase additives and solid-phase extracts. *Rapid Commun Mass Spectrom.* 2004;18(1):49–58.
53. Certo M, et al. Understanding lactate sensing and signalling. *Trends Endocrinol Metab.* 2022;33(10):722–35.
54. Czauderna M, Kowalczyk J. Lactic acid can be easily and precisely determined by reversed-phase high performance liquid chromatography with pre-column derivatization. *J Anim Feed Sci.* 2008;17(2):268–179.
55. Gao S, et al. Comparative Peptidomics analysis of milk fermented by *Lactobacillus helveticus*. *Foods.* 2022;11(23):3885.
56. Tonolo F, et al. Identification of new peptides from fermented milk showing antioxidant properties: mechanism of action. *Antioxid (Basel).* 2020;9(2):117.
57. Sanjulian L, et al. Investigating the Dietary Impact on Trans-Vaccenic acid (Trans-C18:1 n-7) and other beneficial fatty acids in breast milk and infant formulas. *Foods.* 2024;13(14):2164.
58. Liu D, et al. Indoleacrylic acid produced by *Parabacteroides distasonis* alleviates type 2 diabetes via activation of AhR to repair intestinal barrier. *BMC Biol.* 2023;21(1):90.
59. Liu J, et al. Combinational antibacterial activity of Nisin and 3-Phenyllactic acid and their co-production by Engineered *Lactococcus lactis*. *Front Bioeng Biotechnol.* 2021;9:612105.

60. Golubev VI, et al. Antifungal cellobiose lipid secreted by the epiphytic yeast *Pseudozyma graminicola*. *Mikrobiologija*. 2008;77(2):201–6.
61. Rogers KS, Evangelista SJ. 3-Hydroxykynurenine, 3-hydroxyanthranilic acid, and o-aminophenol inhibit leucine-stimulated insulin release from rat pancreatic islets. *Proc Soc Exp Biol Med*. 1985;178(2):275–8.
62. Francisco-Marquez M, Aguilar-Fernández M, Galano A. Anthranilic acid as a secondary antioxidant: implications to the inhibition of OH production and the associated oxidative stress. *Comput Theor Chem*. 2016;1077(1):18–24.
63. Giles GI, et al. Electrochemical and in vitro evaluation of the redox-properties of kynurenine species. *Biochem Biophys Res Commun*. 2003;300(3):719–4.
64. Ramírez-Ortega D, et al. 3-Hydroxykynurenine and 3-Hydroxyanthranilic acid enhance the Toxicity Induced by Copper in Rat Astrocyte Culture. *Oxid Med Cell Longev*. 2017;2017:2371895.
65. Zhuravlev AV, et al. Antioxidant properties of Kynurenines: Density Functional Theory calculations. *PLoS Comput Biol*. 2016;12(11):e1005213.
66. Zheng H, et al. C-Reactive protein and the kynurenic acid to quinolinic acid ratio are independently associated with white matter integrity in major depressive disorder. *Brain Behav Immun*. 2022;105:180–9.
67. Huang L, et al. Two modes of riboflavin-mediated Extracellular Electron transfer in *Geobacter uraniireducens*. *Front Microbiol*. 2018;9:2886.
68. Savitz J, et al. The kynurenine pathway: a finger in every pie. *Mol Psychiatry*. 2020;25:131–47.
69. Delphine O, et al. Histidine is involved in coupling proton uptake to electron transfer in photosynthetic proteins. *Eur J Cell Biol*. 2010;89(12):983–9.
70. Liao SM, et al. The multiple roles of histidine in protein interactions. *Chem Cent J*. 2013;7(1):44.
71. Beetham CM, et al. Histidine transport is essential for the growth of *Staphylococcus aureus* at low pH. *PLoS Pathog*. 2024;20(1):e1011927.
72. Molenaar D, et al. Generation of a proton motive force by histidine decarboxylation and electrogenic histidine/histamine antiport in *Lactobacillus buchneri*. *J Bacteriol*. 1993;175(10):2864–70.
73. Wang X, et al. Immobilization of functional nano-objects in living engineered bacterial biofilms for catalytic applications. *Natl Sci Rev*. 2019;6(5):929–43.
74. Jung S, Chang JY, Lee JH. Arginine metabolism and the role of arginine deiminase-producing microorganisms in kimchi fermentation. *Heliyon*. 2022;8(11):e11802.

Publisher's note

Springer Nature remains neutral with regard to jurisdictional claims in published maps and institutional affiliations.